

STRONG INTERACTIONS AT HIGH ENERGIES

N. G. BIRGER, V. D. MIKHAILOV, I. L. ROZENTAL', and L. I. SARYCHEVA

Usp. Fiz. Nauk 79, 523-544 (March, 1963)

I. INTRODUCTION

STRONG interaction processes involving high-energy particles are, at present, a subject of increasing interest to physicists. It might be said that two factors are responsible for this. One is the rapid progress of accelerator technique, which is extending the range of energies accessible to accurate measurement. Another factor is that the development during the past few years of new methods different from the usual methods of quantum field theory has given rise to some hopes for ending the long-lasting crisis in the theory of strong interactions. We have in mind the theoretical trend based on the use of the most general properties of the fundamental scattering matrix (S matrix). Among these general properties, we should include, above all, the local nature of the interaction, analyticity, and unitarity.* The analytic properties of the S matrix lie at the basis of the dispersion relations for the scattering amplitudes. It should be stressed that at the present time the dispersion relations are the most promising method of the theory of strong interactions.

The complete system of dispersion relations together with the unitarity condition could, perhaps, form a new theory. Thus far, however, such a system has not been found. Even if it were found, there would still arise the far from simple questions of the existence and specific form of its solution. At the present time, there are only the individual dispersion relations. However, it has already proved possible to draw conclusions from them on the asymptotic behavior of the amplitudes for some high-energy processes (see, for example, [2,3]). For this, the so-called double dispersion relations (over two variables: the energy and the momentum transfer) introduced by Mandelstam [4] were used.

It is important to note that this theory already leads to a number of conclusions that can be verified experimentally, in particular, for interactions of particles at high energies. The aim of the present article is to analyze the experimental data on high-energy interactions and to compare them with the theoretical predictions. †

*These questions have been considered in greater detail in the review article.[1]

†This area of interest has been developing with unusual rapidity. The present article reflects the state of the question up to the time of writing (August, 1962).

II. BASIC RESULTS OF THE THEORY

In this section, we present those basic conclusions of the theory in the high-energy region which can be verified experimentally (at least, in principle). We also present here some results obtained from the application of ordinary quantum field theory to strong interactions. These results refer to cases in which the theory is applicable.

1. Pole approximation. Although the unsuitability of the initial meson theories in the region of small distances was obvious, the hope has persisted that, at sufficiently large distances, the ordinary field methods were in a state to give a correct description of strong-interaction processes. This view was reflected in the method of Chew and Low [5] for calculating the cross sections of a strong-interaction process when the interaction proceeds through the exchange of one virtual particle. In this case the amplitude $A(t)$, as a function of the square of the 4-momentum transfer $t = (p_1 - p_2)^2$, has a pole* at $t = m^2$ (m is the mass of the exchanged virtual particle, p_1 and p_2 are the 4-momenta of the particle before and after collision):

$$A(t) = \frac{A_1}{t - m^2} + A_2(t), \quad (2.1)$$

where A_2 are nonpole terms which are neglected. Since $t < 0$ in the physical region, the position of the pole will always lie in the unphysical region for t and the further t lies from the pole m^2 , the greater the role played by the nonpole terms in expression (2.1). †

Berestetskiĭ and Pomeranchuk considered inelastic processes for the conversion of two particles into three particles and two particles into four particles at high energies in the one-pole approximation. [7] They restricted themselves to small momentum transfers $|t| \lesssim m_\pi^2$. It turned out that if the total cross section is constant at high energies, the inelastic cross section for the conversion of two particles into four particles increases logarithmically with the energy and the cross section for the conversion of two particles into three remains constant. This is not in agreement with the initial assumption that the total cross section is constant. However, no contradiction arises if it is assumed that the total cross section decreases like $1/\ln E$.

If the cross section actually does remain constant,

*We employ the system of units in which $\hbar = c = 1$.

†With the aid of this method, we can estimate the cross sections for peripheral processes (see, for example, [6,8,21]).

then there are apparently some factors which limit the applicability of the pole method in the given case.

With the aid of the dispersion relations Gribov^[2] also arrived at the conclusion that the cross section behaves like $1/\ln E$. As regards the applicability of the pole method to processes at very high energies ($E \rightarrow \infty$), it is worthwhile noting that in^[21] this method was shown to be in contradiction with the unitarity condition at high energies (the partial cross section diverges like $\ln E$).

2. Method of complex orbital angular momenta.

Considerable interest has been shown recently in an approach to strong interactions based on the study of the properties of the amplitudes as functions of the orbital angular momentum l in the complex plane l . The initial work in this direction was done by Regge.^[9] Regge studied the analytic properties of the solution to the nonrelativistic Schrödinger equation in the complex plane l and showed that the behavior of the scattering amplitude at high momentum transfers is determined by the position of the pole of the partial wave amplitude in the plane of the angular momentum l . The amplitude then has the form $f(s)t^{l_0}$, where $s = (p_1 + q_1)^2$ and $l_0 = l_0(t)$ is the position of the pole.* Further work^[10,11] showed that in the relativistic case, the partial wave amplitudes are also analytic functions of the angular momentum l and a situation similar to nonrelativistic theory can arise for the asymptotic behavior at large s , i.e., it was shown that the asymptotic behavior of the amplitude at high energies is given by

$$\text{Im } A \sim f(t) s^{l_0(t)}. \quad (2.2)$$

The obtained asymptotic behavior does not correspond to the ordinary diffraction picture.^[10,12] In the classical diffraction picture, the scattering amplitude has the form

$$A(s, t) = sf(t). \quad (2.3)$$

A study of the analytic properties of the amplitude on the basis of the Mandelstam representation showed that the asymptotic behavior of the form (2.3) is difficult to reconcile with the conditions of unitarity and analyticity (Gribov^[2]). At the same time, as was shown by Froissart,^[13] it follows from the unitarity condition and the Mandelstam representation that

$$|A(s, 0)| < Cs \ln^2 s, \quad (2.4)$$

which, by virtue of the optical theorem $\text{Im } A(s, 0) = \sigma$, imposes the following restriction on the asymptotic behavior of the total cross section:

$$\sigma(s) < C \ln^2 s. \quad (2.5)$$

By virtue of (2.2), we find that $l_0(0) \leq 1$. Setting $l_0(0)$

*The quantity s is the square of the total energy of the particles in the center-of-mass system, i.e., $s \sim E_0$, where E_0 is the energy of the incident particle in the laboratory system.

$= 1$, which corresponds to the assumption that the total cross section is constant, we can obtain for small $t < 0$ an expression for the imaginary $A_1(s, t)$ and real $D(s, t)$ parts of the amplitude ($t \approx -1/\ln s$):

$$\begin{aligned} A_1(s, t) &= C s e^{\gamma t \ln s}, \\ D(s, t) &= C s (-\gamma t) e^{\gamma t \ln s}, \quad \gamma > 0. \end{aligned} \quad (2.6)$$

Such an asymptotic behavior of the amplitude leaves the total cross section for high-energy interactions constant, since $A_1(s, 0) = Cs$. At the same time, the diffraction peak shrinks like $|t| \approx 1/\ln s$, and the elastic scattering cross section tends to zero like $1/\ln s$ (see^[12]).* The cross section for inelastic processes then tends to the constant limit

$$\sigma^{\text{in}} = \sigma \left(1 - \frac{a}{\ln s} \right), \quad (2.7)$$

where a is a constant. In this picture, the behavior of the partial amplitudes $a_l(s)$ as functions of the energy also considerably differs from the diffraction picture. In ordinary diffraction, we have $a_l(s) \approx 1$ for sufficiently small l ($l \leq p/m$), but for $l > p/m$, the amplitudes $a_l(s)$ drop rapidly. In the picture outlined above, the amplitudes decrease like $a_l(s) \approx 1/\ln s$ for $l \lesssim (p/m)(\ln s)^{1/2}$ and drop rapidly for $l > (p/m)(\ln s)^{1/2}$. We obtain a picture in which the effective radius of the particles increases with the energy, while the particles become more transparent.^[10]

3. Relations between the cross sections. Nuclear cross sections. The unitarity condition obtained by Gribov^[10] for complex l permits us to write certain relations between the cross sections for various processes in which strongly interacting particles take part. Thus, it was shown in^[14] that for spinless particles we have the relation

$$\sigma_{\pi K}^2 = \sigma_{\pi\pi} \sigma_{KK}, \quad (2.8)$$

where $\sigma_{\pi\pi}$, σ_{KK} , and $\sigma_{\pi K}$ are the total cross sections for interactions between pions, between kaons, and between pions and kaons. Relations of this type can also occur for particles with spin, for example,

$$\sigma_{\pi N}^2 = \sigma_{\pi\pi} \sigma_{NN}. \quad (2.9)$$

Moreover, the following general theorem is valid:

$$\sigma_{AB} \sigma_{CD} = \sigma_{DB} \sigma_{AC}. \quad (2.10)$$

These relations have not yet been verified experimentally, since all strongly interacting particles apart from the nucleon are unstable. However, as was shown in^[14], we can obtain in the same way a similar relation between cross sections for photons and nucleons:

$$\sigma_{\gamma N}^2 = \sigma_{\gamma\gamma} \sigma_{NN}, \quad (2.11)$$

which can, in principle, be verified experimentally.

The foregoing relations between cross sections of strong processes were also obtained in^[15] with the

*See also^[22].

aid of scattering-matrix theory. It was shown that the following relation holds for the total cross sections of nucleon-nucleon scattering σ_{NN} , nucleon-nucleus scattering σ_{NA} , and nucleus-nucleus scattering σ_{AA} at high energies:

$$\sigma_{NN}\sigma_{AA} = \sigma_{NA}^2. \quad (2.12)$$

It is clear that this relation is in contradiction with a dependence of the cross sections on the atomic number A of the form

$$\sigma_{NA} \propto A^{2/3} \quad \text{and} \quad \sigma_{AA} \propto A^{2/3}.$$

As was mentioned above, however, it is also possible to have a physical picture whereby the nucleon radius and transparency both increase with the energy. Then at very high energies, we would evidently have the law

$$\sigma_{NA} \propto A \quad \text{and} \quad \sigma_{AA} \propto A^2, \quad (2.13)$$

which agrees with (2.12). This asymptotic behavior of the nuclear cross sections should occur at much higher energies than in the case of the asymptotic behavior of the cross sections for "elementary" particles.

The asymptotic behavior of the nuclear cross sections was also investigated by Gell-Mann and Udagonkar.^[16] They assumed that at sufficiently high energies ($\gg 1$ GeV), the nucleon-nucleus interaction can be considered quasi-classically, where the incident nucleon interacts independently with the individual nucleons of the nucleus; their motion in the nucleus is neglected. In the case of a complex nucleus, the total cross section turns out to be $\sigma_{NA} = A\sigma_{NN}$ minus the so-called "shadow" correction, which turns out to be proportional to $1/\ln s$, i.e., tends to zero with increasing energy.

Rough numerical approximations for the asymptotic limit of the inelastic cross section^[16] yield the values presented in Table I.

As is seen, even for light nuclei, a very high energy is required before the increase in the inelastic cross section is readily observed. However, Gell-Mann and Udagonkar^[16] believe that for cosmic-ray energies the effect can be considerable and predict that σ_{NA}^{in} for air in the 10^{15} eV region is 25% higher than at 10 GeV. However, the assumption concerning the independence of the individual nucleons in the nucleus is questionable. Hence, the mechanism for the transition from the $\sigma_{NA} \propto A^{2/3}$ dependence to the $\sigma_{NA} \propto A$ dependence is not yet fully explained.

4. **Pomeranchuk's Theorem.** One of the important achievements of the theory of high-energy processes proved to be the theorem formulated by Pomeranchuk^[17] concerning the comparative behavior of the total cross sections of particles and antiparticles at high energies. It was shown that the total cross sections for particles and antiparticles become equal at sufficiently high energies. It was assumed that the total cross sections tend to a constant limit.

Table I

	$E_{\text{lab}}, \text{ GeV}$	10	10^8	10^6	10^9	Asymptotic limit
$A=12$	$\sigma_{NA}^{\text{in}}/\pi R_A^2$	0.98	1.10	1.22	1.23	2.29
$A=216$	$\sigma_{NA}^{\text{in}}/\pi R_A^2$	1.05	1.14	1.24	1.32	6

However, the energy at which the asymptotic region begins and the way the cross sections approach their limit remain unclear.

Recently, it has become possible to say something about what is called the "rate" at which Pomeranchuk's theorem is fulfilled as a function of the energy. As was shown above, the asymptotic behavior of the cross sections is determined by the Regge pole $l_0(t)$, which has the greatest value of $\text{Re } l_0$. Chew and Frautschi showed^[18] that in the relativistic theory the unitarity condition imposes an upper limit on the value of this pole, so that $l_{0\text{max}}(0) = 1$. Hence, this pole, called the vacuum pole by Chew and Frautschi (since the state it determines corresponds to the quantum numbers of the vacuum), should, roughly speaking, determine the asymptotic behavior. However, there also exist other poles corresponding to different particles and resonances which have the quantum numbers of the η , ρ , ω , and π mesons, etc. Since the vacuum pole has the maximum value $l_0(0)$, ensuring the constancy of the total cross section as $E \rightarrow \infty$, the remaining poles determine corrections for energies $E < \infty$. If the investigated process when considered in the crossed (annihilation) channel is characterized by the same quantum numbers as the poles l_i , then the asymptotic cross section will have the form

$$\sigma \sim \text{const} + \sum_i \frac{C_i}{E^{1-l_i(0)}}, \quad (2.14)$$

where E is the energy of the particle in the laboratory system and i is an index denoting poles other than the vacuum pole. Thus, considering interactions between pions and protons, we obtain

$$\sigma_{\pi^-\text{p}} - \sigma_{\pi^+\text{p}} \sim \frac{1}{E^{1-l_\rho(0)}}, \quad (2.15)$$

where l_ρ is a pole corresponding to the ρ meson. We can obtain other relations for various cross sections as well:^[19]

$$\sigma_{\pi^+\text{p}} + \sigma_{\pi^-\text{p}} \sim \frac{a}{E^{1-l_{\text{vac}}(0)}} + \frac{b}{E^{1-l_{ABC}(0)}} = a + \frac{b}{E^{1-l_{ABC}(0)}}$$

(where l_{ABC} is the pole corresponding to the resonance observed by Booth et al^[20]); and also

$$\sigma_{K^-\text{p}} - \sigma_{K^+\text{p}} \sim \frac{c}{E^{1-l_\eta(0)}} + \frac{d}{E^{1-l_\omega(0)}} + \frac{e}{E^{1-l_\rho(0)}},$$

$$\sigma_{K^-\text{p}} + \sigma_{K^+\text{p}} \sim \text{const} + \frac{1}{E^{1-l_{ABC}(0)}},$$

$$\sigma_{\bar{p}p} - \sigma_{pp} \sim \frac{f}{E^{1-l_\pi(0)}} + \frac{g}{E^{1-l_\omega(0)}} + \frac{i}{E^{1-l_\rho(0)}},$$

$$\sigma_{\bar{p}p} + \sigma_{pp} \sim \text{const} + \frac{l}{E^{1-l_\pi(0)}} + \frac{m}{E^{1-l_{ABC}(0)}},$$

where l_π , l_ω , and l_ρ are poles corresponding to the π , ω , and ρ mesons; c, d, e, f, g, i, l, and m are certain constants. In this way, we obtain an interesting relation for the dependence of the cross sections for interactions of particles and antiparticles with nucleons as a function of the energy and position of the poles corresponding to elementary particles (resonances). The values of these poles can be found with the aid of the experimental data on the cross sections.

III. CROSS SECTIONS FOR THE INTERACTION OF PIONS AND NUCLEONS BETWEEN 2 AND 28 GeV

In this section, we compare the data obtained in accelerator experiments with the theoretical predictions presented in the preceding section. We shall make use here of accelerator experiments performed in 1961-1962. Earlier data are contained in a number of review articles (see, for example, [23]).

1. Total cross sections for interactions of particles and antiparticles with protons. Recent measurements of the total cross sections for interactions of particles and antiparticles with protons employed mainly two techniques: a) counter arrangements, b) bubble chambers. The first method permits the accumulation of much larger statistics than the second, and we shall therefore use the data obtained by the first method.

Figure 1 shows a typical arrangement taken from [24] (similar arrangements were used in all the remaining experiments). A beam of secondary particles produced in an internal target of the accelerator is momentum-analyzed with the aid of a deflecting magnet and is focused by quadrupole lenses (not shown in the figure) at the center of a Cerenkov counter C. The Cerenkov counter separates particles of a given mass. The secondary particles produced in the walls of the collimator, in air, and in the Cerenkov counter are cleared from the beam by the bending magnet B_2 . The

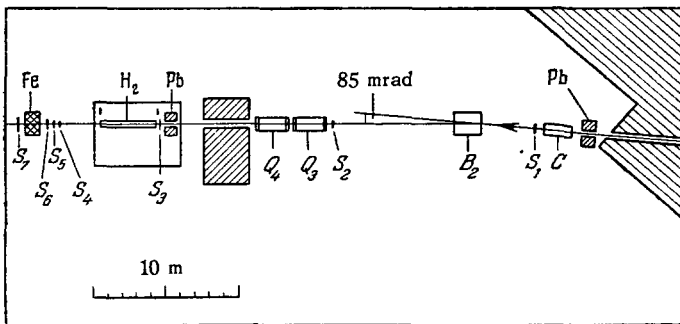


FIG. 1. Arrangement for determination of proton total cross sections.

quadrupole lenses Q_3 and Q_4 then focus the beam on counters S_4 - S_6 located behind a liquid-hydrogen target. The $(S_1S_2S_3CS_i)$ coincidences (where $i = 4, 5,$ and 6 denote the counters placed after the target) and $(S_1S_2S_3C)$ coincidences are recorded. To take into account the number of interactions produced in the walls of the liquid-hydrogen vessel, measurements are also made of coincidences when the hydrogen target (H_2) is replaced by steel plates simulating the walls of the vessel ("empty" target). Hence, in such an experimental arrangement, we measure the fraction of particles traversing the hydrogen target without interaction, except for cases of scattering by small angles. To introduce a correction for such events, the dependence of the number of coincidences on the solid angle obtained by means of counters S_4 , S_5 , and S_6 is extrapolated to zero angle. The angles subtended by the counters are chosen to be sufficiently small so as to permit a linear extrapolation of the differential cross section $d\sigma/d\Omega$ to zero solid angle.

To illustrate the mass resolution given by a Cerenkov counter, Fig. 2 shows the mass spectrum of negative particles of momentum* 8 GeV obtained in a similar arrangement. [25] The fraction of kaons and antiprotons is between 0.5 and 2% in the 3-10 GeV momentum interval.

To obtain the absolute values of the total cross section, it is necessary to introduce several corrections (apart from those mentioned above):

- a) Correction for Coulomb scattering of beam particles in the target; this correction is most important for the smallest measured momenta (thus, for example, at 4 GeV the correction is $\approx 1\%$).
- b) Corrections for the contamination from particles of another mass [for example, muons ($\approx 2-3\%$) and electrons ($\approx 1\%$) in the pion beam].

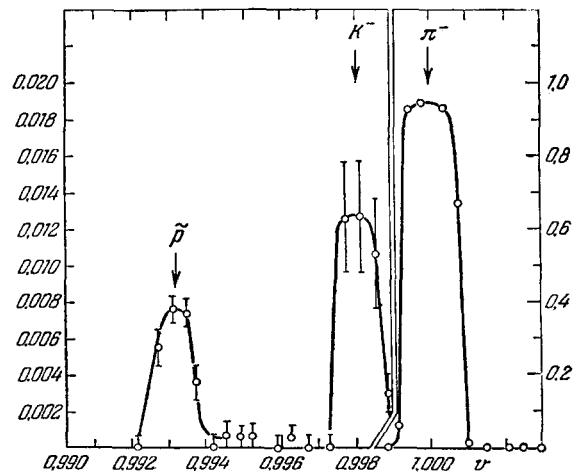


FIG. 2. Negative particle mass spectrum. The velocity of particles of 8-GeV momentum is given on the abscissa axis.

*We recall that $c = \bar{n} = 1$.

c) In the case of the measurement of σ_{K^\pm} , it is necessary to introduce corrections for the change in the number of decays in flight connected with the ionization losses in the target.

d) Other possible errors in the absolute cross-section measurements can be due to the uncertainty in determining the effective length of the target, calibration of the "empty" target, etc.

It should be mentioned that most of the systematic errors enumerated above, except for (b), do not affect the difference between the particle and antiparticle cross sections.

A. σ_{pp} and $\sigma_{\bar{p}p}$. The principal results were obtained in [24,26]. The π^- -meson contamination in the antiproton beam was $\approx 1\%$ at small momenta and $\approx 0.2\%$ at a momentum of 20 GeV.

Figure 3 shows data for σ_{pp} and $\sigma_{\bar{p}p}$ in the 2–24 GeV momentum interval. For σ_{pp} , we have data up to 28 GeV. [27] The errors shown in the figure include both the statistical and systematic errors enumerated above.

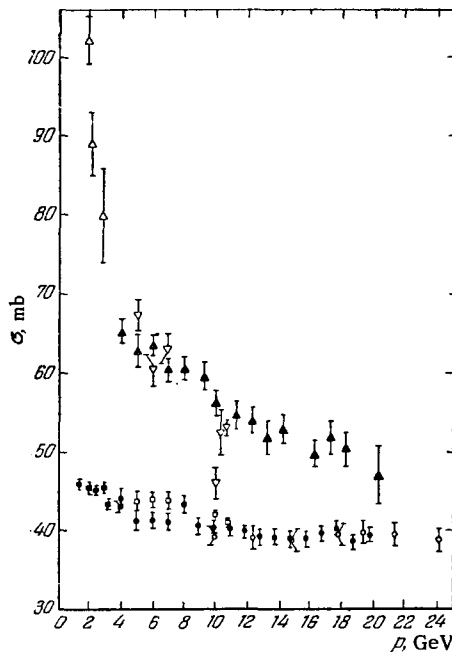


FIG. 3. Total cross section for p-p and \bar{p} -p interactions. $\sigma_{\bar{p}p}$: ∇ - data of [24], \blacktriangle - data of [26], Δ - data of [26]; σ_{pp} : \square - data of [24], \bullet - data of [26], \circ - data of [27], \blacksquare - data of [27].

The values of the total cross sections and the difference $\Delta = \sigma_{\bar{p}p} - \sigma_{pp}$ for various momenta are shown in Table II. In the 10–20 GeV momentum interval, the value of σ_{pp} has been measured in intervals of 1 GeV. The cross section remained constant within the limits of error ($\approx 2.5\%$) and proved to be

$$\bar{\sigma}_{pp} \Big|_{10 \text{ GeV}}^{20 \text{ GeV}} = (39.5 \pm 0.3) \text{ mb.}$$

This also holds up to 28 GeV with somewhat poorer accuracy ($\approx 4\%$). At the same time, in the 6–20 GeV

Table II

σ , mb	p , GeV		
	6	10	20, 3
$\sigma_{\bar{p}p}$	65 ± 4	58 ± 4	48 ± 4
σ_{pp}	41 ± 1.5	39.5 ± 1.0	39.5 ± 1.0
Δ	24 ± 4.2	18.5 ± 4.1	8.5 ± 4.1

momentum interval, the difference in the cross sections for protons and antiprotons decreases with increasing momentum like A/p , where $A \approx 170 \text{ mb-GeV}$. If such behavior with the energy is also maintained at larger values of E , then Pomeranchuk's theorem for protons and antiprotons should be fulfilled to an accuracy of $\approx 1\%$ at energies of $\approx 1000 \text{ GeV}$.

B. σ_{π^-p} and σ_{π^+p} . The principal results belong to two groups as in the case of the proton and antiproton cross-section data. The full interval of measured momenta is 4.5–20 GeV. [25,28,29] The data for both groups, including data at smaller momenta, are shown in Fig. 4.

Table III lists the values of $\sigma_{\pi^\pm p}$ and the difference Δ for various momenta averaged over the data of [25,28,29].

It is seen from Table III and Fig. 4 that in the momentum interval under consideration, a dependence on the momentum is observed both for $\sigma_{\pi^\pm p}$ and Δ .

If the experimental data on the total cross sections in the 4–20 GeV momentum interval are analyzed by the χ^2 method, a best fit to the function of the form [29] $\sigma_{\pi^\pm p} = \sigma_\infty + b^\pm p^{-\beta}$ is obtained with the values $\beta = 0.7$, $\sigma_\infty = 22.48 \text{ mb}$, $b^- = 22.10 \text{ mb-(GeV)}^{0.7}$, $b^+ = 14.37 \text{ mb-(GeV)}^{0.7}$.

For such a momentum dependence of $\sigma_{\pi^\pm p}$, the difference in cross sections will tend to zero in accordance with the law

$$\Delta = \sigma_{\pi^-p} - \sigma_{\pi^+p} = \frac{a}{p^{0.7}},$$

where

$$a = 8 \text{ mb-(GeV)}^{0.7}.$$

If in the case of π^\pm mesons at higher energies the same energy dependence is preserved for Δ , then Pomeranchuk's theorem will be fulfilled to an accuracy of the order of 1% at an energy of $\sim 100 \text{ GeV}$.

As was shown above (Sec. II.4), the way in which the antiparticle and particle cross sections for interactions with nucleons tend to zero is determined by the values of the Regge poles at the point $t = 0$ corresponding to the quantum numbers of the known particles or resonances:

$$\sigma_{\pi^-p} - \sigma_{\pi^+p} \sim \frac{1}{E^{1-l_\rho(0)}},$$

where E is the energy in the laboratory system and l_ρ is the Regge pole with quantum numbers of the ρ meson ($T = 1$, $G = 1^+$). From comparison with experimental data, we obtain $l_\rho(0) \sim 0.3$.

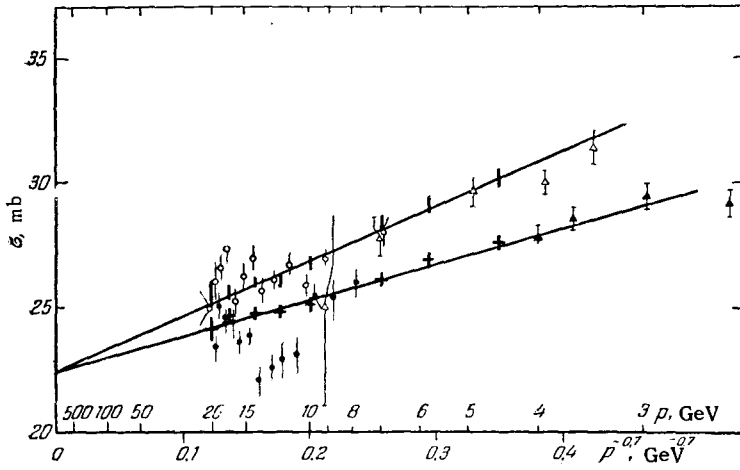


FIG. 4. Total cross section for π^- -p and π^+ -p interactions. σ_{π^-p} : ■ - data of [25,29], ○ - data of [26], Δ - data of [46]; σ_{π^+p} : + - data of [25,29], ● - data of [28], ▲ - data of [47].

Table III

σ , mb	p , GeV					
	4,5	7	10	14	17	20
σ_{π^-p}	30.2 ± 0.4	28.4 ± 0.4	26.7 ± 0.35	26.0 ± 0.2	25.8 ± 0.3	25.5 ± 0.4
σ_{π^+p}	27.6 ± 0.3	26.1 ± 0.3	25.1 ± 0.4	24.7 ± 0.3	24.3 ± 0.3	23.8 ± 0.4
Δ	2.6 ± 0.5	2.3 ± 0.5	1.6 ± 0.55	1.3 ± 0.35	1.5 ± 0.4	1.7 ± 0.6

C. σ_{K^-p} and σ_{K^+p} . Figure 5 shows the data for the K^- -p and K^+ -p total cross sections. [25,30,31] There is no information on the values of these cross sections at the present time.

For momenta > 5 GeV, a slow decrease in $\sigma_{K^\pm p}$ is observed with increasing energy. The difference in the cross sections Δ does not change, within the limits of experimental error, in the 8–13 GeV momentum interval and is equal to 5 ± 2 mb, which is $\approx 25\%$ of σ_{K^-p} at 13 GeV.

Hence, for all strongly interacting particles whose total cross sections for interactions with protons have been measured up to momenta of 20–30 GeV, Pomereanchuk's theorem is not strictly fulfilled. However, both the dependence of the total cross sections on the energy and the change in the difference of the cross

sections for antiparticles and particles display a tendency to fulfill this theorem at high energies ($\gtrsim 100$ GeV).

2. Elastic scattering of protons and pions. Elastic scattering of protons and pions on nucleons is investigated mainly by three techniques: 1) counter measurements, 2) bubble chambers, 3) nuclear emulsions.

The greatest statistics can be obtained by the first method, but until now this method has been used to obtain data only on p-p scattering, owing to the necessity of identifying the nature of the particles when π -N scattering is studied. All techniques make use of the kinematic relations between the momenta and angles of the scattered particles to distinguish elastic scattering from inelastic processes.

A. p-p scattering. Analyses of the data on p-p elastic scattering have been made by several authors, for example, [32]. We consider only the experimental

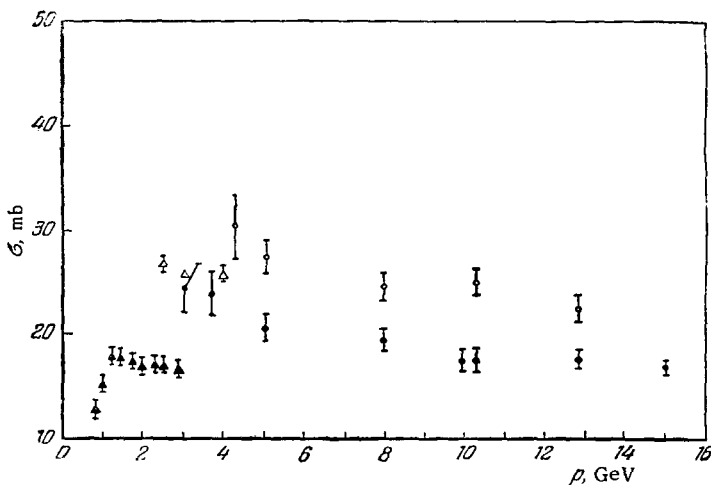


FIG. 5. Total cross section for K^- -p and K^+ -p interactions. σ_{K^-p} : Δ - data of [30], ○ - data of [31]; σ_{K^+p} : ● - data of [31], ▲ - data of [9].

data that can be analyzed from the viewpoint of the theory discussed in Sec. II.2.

Using formula (2.2), we write the dependence of the angular distribution for elastic scattering in the forward direction on the energy s and the square of the momentum transfer t ; for $s \rightarrow \infty$ and $t \ll s$, we have

$$\frac{d\sigma^{el}}{dt} = \frac{\pi}{k^2} \frac{d\sigma^{el}}{d\Omega} = |f(t)|^2 s^{2[l_0(t)-1]}. \quad (3.1)$$

Here, $t = -2k^2(1 - \cos \theta)$, k is the wave number, and θ is the scattering angle, $d\sigma^{el}/d\Omega$ is the differential cross section for scattering into an element of solid angle ($d\Omega = 2\pi \sin \theta d\theta$) in the center-of-mass system.

It follows from formula (3.1) that the diffraction peak shrinks with increasing energy of the scattered particles. With an increase in t , the difference in the cross sections $d\sigma^{el}/dt$ at different energies increases, so that $l(t)$ should, according to the theoretical predictions, decrease with increasing t [$l_0(0) = l_0 \text{ max} = 1$]; at small t the quantity $d\sigma^{el}/dt$ weakly depends on t . Since the experimental data agree qualitatively with the dependence of $d\sigma^{el}/dt$ on s predicted by the theory, the authors of [33] determined the values of the function $l(t)$. For this, they used data yielding the best statistical accuracy for the angular distribution and the broadest interval of measured values of t ($0.2-2.5 \text{ GeV}^2$) and s ($7.7-5.4 \text{ GeV}^2$). [34,35] In [34], both scattered protons were recorded; in [35], the momenta of the fast protons scattered at a fixed angle were measured. Figure 6 shows the obtained angular distribution. The value of $d\sigma^{el}/dt$ at $t = 0$ was determined from the optical theorem under the assumption that the real part of the scattering amplitude at these energies is zero; σ was taken equal to 40 mb for all energies. Using the data of Fig. 6, we can determine the numerical values of the function $l_0(t)$. From formula (3.1), we obtain

$$l_0(t) = 1 + \frac{\log \frac{d\sigma^{el}(s_1)}{dt} - \log \frac{d\sigma^{el}(s_2)}{dt}}{2(\log s_1 - \log s_2)}. \quad (3.2)$$

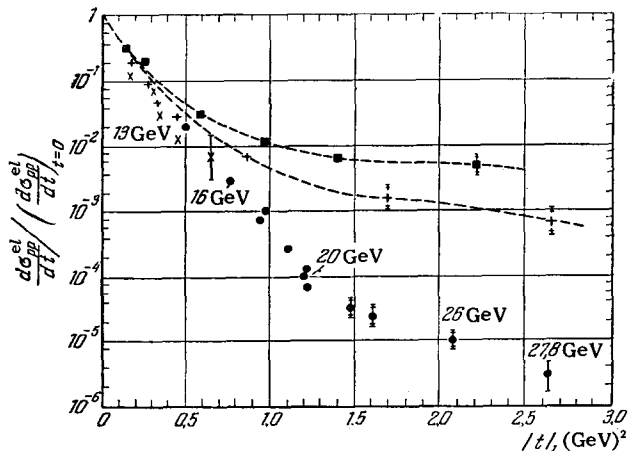


FIG. 6. Differential cross section for p-p elastic scattering as function of the square of the momentum transfer t . ■ — 3.04 GeV, from [34]; + — 5.25 GeV, from [34]; × — 7.02 GeV, from [34]; ● — from [35].

The function $l_0(t)$ is shown in Fig. 7.

Figure 8 presents the data on the total cross section for elastic scattering σ^{el} as a function of the energy. [34,36,40] It is seen from the figure that, within the limits of experimental error, σ^{el} does not change in the energy interval between 4 and 24 GeV. The statistical accuracy of the results does not make it possible to exclude the logarithmic dependence of σ^{el} on E in this interval, which is predicted by the theory (Sec. II).

B. π -N scattering. To verify the correctness of the theoretical predictions, it would be very important to find independently the function $l_0(t)$ for the case of π -N scattering, since $l_0(t)$ is a universal function describing the forward scattering of all strongly interacting particles.

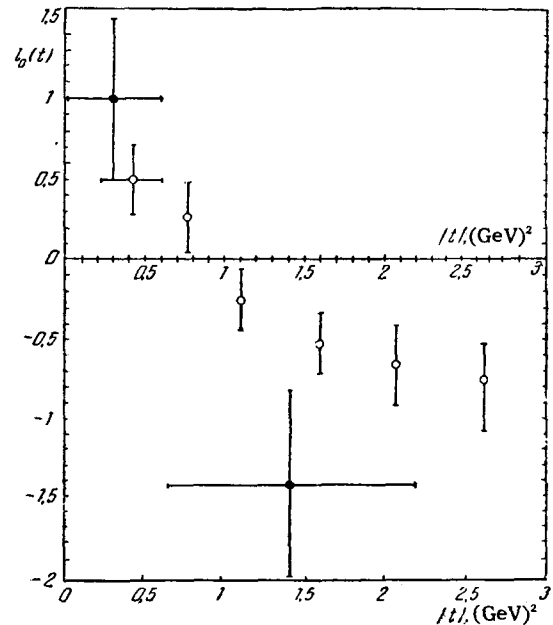


FIG. 7. The function $l_0(t)$. ○ — p-p scattering; ● — π -N scattering.

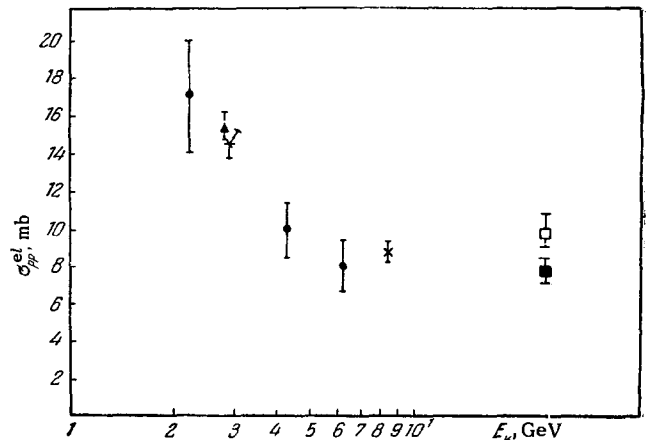


FIG. 8. Total cross section for p-p elastic scattering. ● — data of [34]; ▲ — data of [36]; + — data of [37]; × — data of [38]; ■ — data of [39]; □ — data of [45].

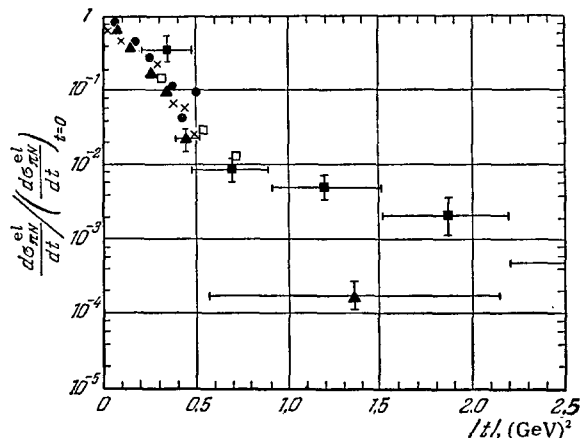


FIG. 9. Differential cross section for π -N elastic scattering as function of the square of the momentum transfer t . ■—2.8 GeV, from [42]; ●—2.8 GeV, from [42]; ▲—5.1 GeV, from [43]; ×—6.8 GeV, from [44]; and □—7.1 GeV, from [45].

Figure 9 shows the results of the determination of $d\sigma^{el}/dt$ at different primary energies [41–45] [$6 < s < 28$ (GeV) 2]. As is seen from the figure, the interval of investigated momenta t is much narrower than for p-p scattering [most of the data were obtained for $t < 0.5$ (GeV) 2], while the errors in the measured differential cross section are much larger than for p-p scattering. This does not permit us to obtain $I_0(t)$ from π -N scattering at the present time, but the numerical values of $I_0(t)$ determined from π -N scattering for two values of t do not appear to be inconsistent with the data for p-p scattering, within the limits of very large errors (see Fig. 7).

IV. PION-NUCLEUS AND NUCLEON-NUCLEUS CROSS SECTIONS AT VERY HIGH ENERGIES

1. Special features of cross-section measurements in cosmic-ray interactions. In this section, we present data on the cross sections obtained in the study of cosmic rays. The cross-section measurements for cosmic-ray particles have the following characteristics:

a) The charge of the target nucleus is always greater than unity, and in some cases as, for example, in nuclear emulsions, which are of very complex composition, it cannot be determined.

b) The energy of the incident particles is estimated only approximately, while the degree of approximation depends on the method of registration. Usually, the energy of the cosmic-ray particles is determined to an accuracy of a factor of ≈ 2 . The most accurate method of determining the energy with the aid of an ionization calorimeter [54] appears to give an error of ≈ 30 –50%

c) It is always the inelastic cross sections that are measured in cosmic-ray experiments. Moreover, none of the existing techniques permit the recording of events with small inelasticity coefficients. Hence, these data give a lower limit of the cross section.

Although the foregoing features make difficult an unambiguous interpretation of the events, it should be stressed that they cannot have an important effect on the final conclusions. For example, the uncertainty in the measurement of the energy is not important (since very large energy intervals are usually considered).

2. Determination of the cross sections in air based on measurement of the absorption of the nucleon component. We consider the experimental data on interactions of nucleons and pions in the energy interval from ≈ 10 to 10^4 GeV with nuclei of air. In Table IV, we list the data on the attenuation length for the nuclear-active particles. A considerable fraction of these particles are apparently nucleons. In fact, from the available data on the multiplicity and distribution of energy between nucleons and pions in an elementary collision, it follows that in the energy interval of interest to us, less pions should be present than nucleons.

Table IV. Attenuation length of high-energy nuclear-active particles in air

Energy, GeV	L_n , g/cm 2	Method of recording nuclear interactions	References
> 470	125	Emulsion at different heights	52
360–5000	119 ± 1	Counters	51
≈ 30	115	Emulsion	49
to 1000	116 ± 9	Counters	50
≈ 1000	131 ± 3		
≈ 100	105 ± 16	Emulsion	53
≈ 3000	115 ± 10		
1000–3000			

Moreover, the experimental data indicate [62,76] that low in the atmosphere, half of the cosmic-ray nuclear-active particles have no charge. This is also evidence against the suggestion that the nuclear-active component contains a large number of pions. From the size of the attenuation length L_n , we can readily estimate the cross section for the interaction of nucleons with nuclei of air. The interaction length L_{int} is connected with the quantity L_n by the following simple relation: [55,56]

$$\frac{L_{int}}{L_n} = 1 - \int_0^1 x^\gamma \varphi(x) dx, \quad (4.1)$$

where $\varphi(x)$ is a function of the distribution of the fraction of energy carried away by the nucleon after the collision and γ is the exponent for the energy spectrum, which is well approximated by an exponential function. The integral in (4.1) depends weakly on the form of the function φ and is quite well determined by a mean inelasticity coefficient equal to 0.3–0.5 on the basis of numerous experimental data.

Assuming that $L_n = 120$ g/cm 2 (see Table IV), we find that $L_{int} \approx 70$ –80 g/cm 2 (330–290 mb).

Another way of determining the cross sections is connected with the recording of the high-energy nuclear-active shower particles (Grigorov et al.^[57] and Zatsepin et al.^[58]). This method involves the measurement of the nuclear-active particle flux without (N_1) and with (N_2) an accompanying shower. Assuming that a particle without an accompanying shower traverses a path l without interaction, we obtain

$$N_1 = N_0 e^{-\frac{l}{L_{\text{int}}}},$$

where N_0 is the particle flux at the boundary of the atmosphere. The total number of particles is $N_1 + N_2 = N_0 \exp(-l/L_n)$. Measuring N_1 and N_2 and choosing some definite value of L_n (see Table IV), we can readily calculate N_0 and L_{int} ; L_{int} turns out to be $\approx 80 \text{ g/cm}^2$.

The cross section for the interaction of fast pions with air nuclei can be estimated on the basis of data on the energy spectrum of high-energy photons. If the depth at which the photons are produced is sufficiently small, then the recordable γ quanta are largely produced directly from π^0 decay. By measuring the energy spectrum of such photons, we can readily establish the spectrum of the neutral pions producing them, and consequently, also the charged-pion spectrum. Then, by simple calculations, we can obtain the number of muons at sea level as a function of L_{int} and L_n . For sufficiently high energies, $E > 10^2 \text{ GeV}$, the number turns out to be^[59]

$$N_\mu = C(E) \frac{L_{\text{int}}}{L_n - L_{\text{int}}} \ln \frac{L_n}{L_{\text{int}}}. \quad (4.2)$$

The results of estimates^[59] of the muon intensity in the 100–5000 GeV energy interval at sea level for values of $L_n \approx 125 \text{ g/cm}^2$ and $L_{\text{int}} = 80 \text{ g/cm}^2$ are shown in Fig. 10, from which it is seen that the calculated intensity is in good agreement with the value obtained by direct measurements. It should be noted that the value of L_{int} determined in this way is essentially an upper limit of this value, since in our derivation, we assumed that the pions are the only source of muons.

3. Determination of the cross sections for interactions of particles at superhigh energies ($> 10^4 \text{ GeV}$). In this case, the main source of our knowledge is data on extensive air showers. Estimates of the interaction cross sections based on analysis of the extensive-air-shower characteristics have been made by many authors. As a rule, some specific model for shower development lies at the basis of the calculation. In^[60,61], the length L_{int} was determined on the basis of the following model. It was assumed that a) after reaching a maximum, the shower is absorbed exponentially like $\exp(-l/L)$ (L is the mean attenuation length range for an extensive air shower of a given size); b) the height of the maximum is determined by the expression $D \ln(E_0 C)$ (D and C are constants); c) the num-

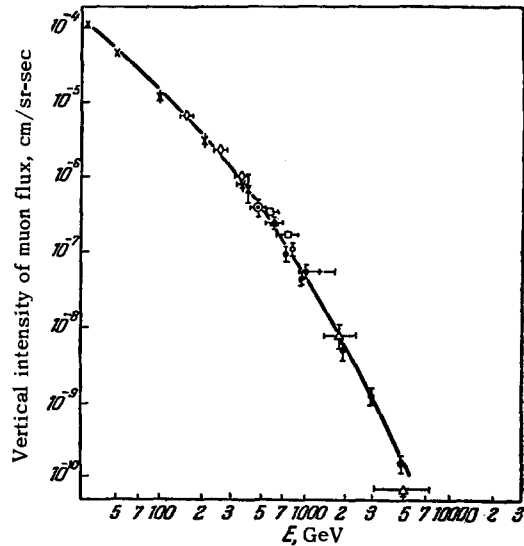


FIG. 10. Experimental data on cosmic-ray muon spectrum. ●— Values calculated from data on the photon spectrum at great heights under the assumption that $L_{\text{int}} = 80 \text{ g/cm}^2$. The remaining points are determined by other methods.

ber of muons in the shower is proportional to the primary energy and their spatial distribution is standard and independent of the energy.* The characteristics of showers calculated from this model depend on three parameters (D , L_{int} , and L). These three quantities are determined by comparison of the results of the calculations with three groups of experimental data: the angular distribution of the showers, their behavior as a function of the height, and the fraction of muons relative to the number of electrons in the showers. The value of L_{int} determined this way is 70–100 g/cm^2 in^[60] and $85 \pm 5 \text{ g/cm}^2$ in^[61]. It should be mentioned, however, that although the assumptions lying at the basis of the conclusion are natural from the qualitative viewpoint, their accuracy is difficult to estimate. The unrestricted approximation of the shower depth variation by an experiment is doubtful. In fact, it is clear, for example, that close to the maximum, the exponential approximation is incorrect. In this connection, estimates made for extensive air showers with 10^5 – 10^6 particles are correct, i.e., for primary particles of energy $E_0 \approx 10^5$ – 10^6 GeV , since these showers are far past the maximum of their development. The depth variation of the showers at higher energies ($\approx 10^7$ – 10^8 GeV) is better described by a Gaussian function close to their maximum than by exponential.^[62] Therefore, for such energies, it is worthwhile having a different approach to the estimate of the upper limit of the L_{int} . Hence we separate the development of the shower into two stages: the first is the interaction of the primary particle with a length L_{int} and the second

*Neglect of fluctuations in the muon spatial distribution can have a significant effect on the estimates of L_{int} determined by this method.

Table V. Attenuation length of extensive air showers as a function of E_0

Method of determination	Number of particles in EAS*	L, g/cm ²
From barometric effect [64]	2·10 ³	138
	8·10 ³	123
	10 ⁴	121
From barometric effect [65]	2·10 ⁴	114
	10 ⁴	114
	3·10 ⁴	122
	9·10 ⁴	94
From barometric effect [66]	3·10 ⁵	100
	3·10 ⁵	114
	8·10 ⁵	110
	2·10 ⁶	111
	5·10 ⁶	110
	10 ⁷	106
From angular distribution measured by scintillation counters [67]	2·10 ⁷	106
	10 ⁸	107
	10 ⁸	98
From angular distribution measured by scintillation counters [68]	10 ⁷	90
	1,2·10 ⁸	121
	8·10 ⁸	111
Averaged results from barometric effect and angular distribution [69]	1,8·10 ⁷	109
	2,7·10 ⁷	141±12
Comparison of number of shower particles at sea level and at 3860 m (data from [70])	10 ⁵	156±22
	3·10 ⁵	125 ⁺¹⁹ ₋₁₉
From angular distribution measured by scintillation counters [71]	8,5·10 ⁵	107 ⁺¹⁷ ₋₁₂

*The energy of the primary particle producing the shower was determined from the relation $E_0 = kN$. The measurements were carried out at sea level, for which $k = 14$ GeV.

is the development of the cascade shower that results from this interaction. In the most general case, the cascade curve can be represented in the form

$$AE_0 \exp \{ -\alpha\xi^2 + \beta\xi^3 + \gamma\xi^4 + \dots \} \quad (\alpha > 0),$$

where $\xi = l - l_{\max}$; here l_{\max} is the depth corresponding to the maximum and A is a constant. The function $\{ -\alpha\xi^2 + \beta\xi^3 + \dots \}$ for $\xi = 0$ has a single maximum.

In the general case, it can be shown that

$$\frac{1}{L} = \frac{1}{L_{\text{int}}} - \frac{dE_{0\text{min}}}{dl} \psi, \quad (4.3)$$

where ψ is an essentially positive quantity and $E_{0\text{min}}$ is the minimum energy of the primary particle producing N secondary particles at the depth of observation. If this depth is sufficiently large so that the shower produced by a particle of energy $E_{0\text{min}}$ is past the maximum, then $dE_{0\text{min}}/dl > 0$. In this case, which practically always occurs, we have $L_{\text{int}} > L$. Formula (4.3), relating the quantities L and L_{int} , reflects the simple fact that the absorption length for shower particles is the upper limit for the interaction range of primary particles. Table V lists data on the attenuation lengths in air for extensive air showers obtained over a very large energy interval. From these data, we note a very distinct tendency for the value of L to decrease with increasing size of the shower. Thus, for an energy $\geq 10^8$ GeV, the length becomes ≈ 100 g/cm². From formula (4.3), it follows that the decrease

in the value of L with increasing energy is, perhaps, connected with the decrease in the second term, which reflects the approximation that was made: that at the given height, the high-energy shower was considered to be at the maximum of its development. There is also another possibility, namely, that the decrease in L by 20% corresponds approximately to the same increase in the inelastic cross section. Unfortunately, however, this conclusion is not unambiguous.

In this way, cross-section data for the interaction of nuclear-active particles with nuclei of air obtained by various methods over a very broad energy interval ($10-10^8$ GeV) provide evidence of the approximate (and, perhaps, strict) constancy of this quantity.*

Figure 11 presents the results of the cross section measurements for interactions of nuclear-active particles with various nuclei over a very broad energy range. We consider it more useful to present data on the cross sections for various nuclei and not to recalculate the data in terms of a nucleon-nucleon cross

*It should be mentioned that the cross section determined from the analysis of data on extensive showers refers, strictly speaking, to the primary particles of cosmic rays. In principle, it is possible, in our view, to put forward the little likely hypothesis that the approximate constancy of the cross section found by the method described above, up to very high energies, reflects a situation in which the effect of the change in the composition of the primary component (increase in the fraction of heavy nuclei with increasing energy E_0) is offset by the decrease in their interaction cross section.

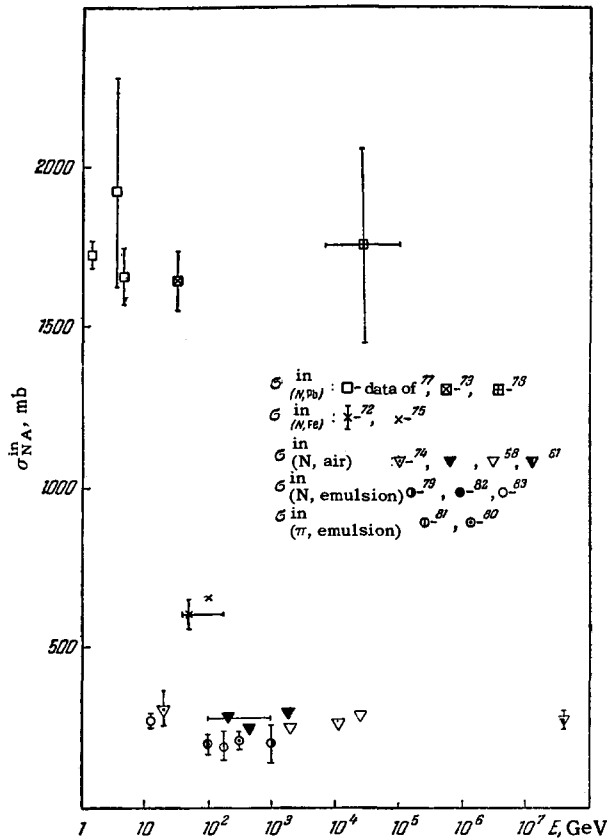


FIG. 11. Inelastic cross section for nuclear-active particles with various elements as a function of the primary particle energy (∇ - from [57]).

$$\bar{\sigma}_{(N, \text{emulsion})}^{\text{in}} = \frac{A^{1/3} s A^{2/3}}{NL}, \quad N = 6.02 \times 10^{23} \text{ (L in g)}.$$

section, which is inevitably based on some not very justified assumption concerning the mechanism for interactions between nucleons and nuclei. [72, 73, 23]

It is seen from the figure that, to an accuracy of about 20%, the cross section for inelastic processes σ_{NA}^{in} does not change.* There exist two possibilities for the change in σ_{NA}^{in} with the energy predicted by the theory: 1) an asymptotic increase in σ_{NA}^{in} similar to that which occurs for nucleon-nucleon interactions in accordance with formula (2.7); 2) an increase in σ_{NA}^{in} with increasing energy of the type indicated in Sec. 2.3, which is due to the specific nature of the interaction with nuclei and the transition with increasing energy from the dependence $\sigma_{NA}^{\text{in}} \propto A^{2/3}$ to the asymptotic dependence $\sigma_{NA}^{\text{in}} \propto A$ as the energy increases. Each of these possibilities leads to a change of ≈ 20 –25% in the cross section in the 10 – 10^7 GeV energy interval. The available experimental data do not contradict such a weak increase, however, their accuracy is not sufficient to enable one to state that the increase is experimentally established.

*The most extreme estimate of the lower limit for the quantity $\bar{\sigma}_{NA}^{\text{in}}$ leads to the conclusion that it does not decrease by more than a third.

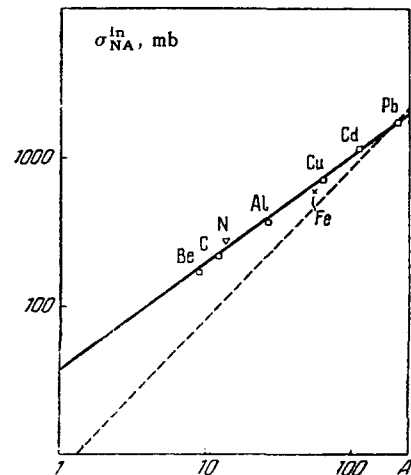


FIG. 12. Variation of inelastic cross section with atomic number. Use was made of results of [27] for Be, C, Al, Cu, Cd, and Pb at 25 GeV and data from [74] for Pb, [75] for Fe, [58] for air at primary particle energies of $\approx (10^2 - 10^4)$ GeV.

As regards the dependence of σ_{NA}^{in} on A at the various energy intervals, the experimental results (Fig. 12) show that up to an energy of $\approx 10^4$ GeV, the cross section is well described by the $A^{2/3}$ law and indicate that the asymptotic behavior does not yet appear at these energies.

¹V. B. Berestetskiĭ, UFN 76, 25 (1962), Soviet Phys. Uspekhi 5, 7 (1962).

²V. I. Gribov, Nuclear Phys. 22, 249 (1961).

³G. Domokos, Joint Institute for Nuclear Research, Preprint D-773, 1961.

⁴S. Mandelstam, Phys. Rev. 112, 1344 (1958).

⁵G. F. Chew and F. E. Low, Phys. Rev. 113, 1640 (1959).

⁶L. B. Okun' and I. Ya. Pomeranchuk, JETP 36, 300 (1959), Soviet Phys. JETP 9, 207 (1959).

⁷V. B. Berestetskiĭ and I. Ya. Pomeranchuk, JETP 39, 1078 (1960), Soviet Phys. 12, 752 (1961).

⁸I. M. Dremin and D. S. Chernavskii, JETP 38, 229 (1960), Soviet Phys. JETP 11, 167 (1960).

⁹T. Regge, Nuovo cimento 14, 951 (1959); ibid 18, 947 (1960).

¹⁰V. N. Gribov, JETP 41, 1395 (1962), Soviet Phys. JETP 14, 1395 (1962).

¹¹V. N. Gribov, JETP 42, 1260 (1962), Soviet Phys. JETP 15, 873 (1962).

¹²V. N. Gribov, JETP 41, 667 (1961), Soviet Phys. JETP 14, 478 (1962).

¹³M. Froissart, Phys. Rev. 123, 1053 (1961).

¹⁴V. N. Gribov and I. Ya. Pomeranchuk, Institute of Theoretical and Experimental Physics, Acad. Sci. U.S.S.R., No. 42, 1962.

¹⁵Gribov, Ioffe, Pomeranchuk, and Rudik, Institute of Theoretical and Experimental Physics, Acad. Sci. U.S.S.R., No. 50, 1962.

- ¹⁶ M. Gell-Mann and B. M. Udgaonkar, *Phys. Rev. Lett.* **8**, 346 (1962).
- ¹⁷ I. Ya. Pomeranchuk, *JETP* **34**, 725 (1958), *Soviet Phys. JETP* **7**, 499 (1958).
- ¹⁸ G. F. Chew and S. C. Frautschi, *Phys. Rev. Lett.* **7**, 394 (1961); *ibid* **8**, 41 (1962).
- ¹⁹ B. M. Udgaonkar, *Phys. Rev. Lett.* **8**, 142 (1962).
- ²⁰ Booth, Abashian, and Crowe, *Phys. Rev. Lett.* **7**, 35 (1961).
- ²¹ F. Salzman and G. Salzman, *Proc. of Intern. Conf. on High-Energy Phenom.*, CERN, 1961, p. 288.
- ²² G. Domokos, *Nuovo cimento* **23**, 1175 (1962).
- ²³ V. S. Barashenkov, *UFN* **72**, 53 (1960), *Soviet Phys. Uspekhi* **3**, 689 (1961).
- ²⁴ von Dardel, Mermod, Piroué, Vivargent, Weber, and Winter, *Phys. Rev. Lett.* **7**, 127 (1961).
- ²⁵ von Dardel, Frisch, Mermod, Milburn, Piroué, Vivargent, Weber, and Winter, *Phys. Rev. Lett.* **5**, 333 (1960).
- ²⁶ Lindenbaum, Love, Niederer, Ozaki, Russel, and Yuan, *Phys. Rev. Lett.* **7**, 185 (1961).
- ²⁷ Ashmore, Cocconi, Diddens, and Wetherel, *Phys. Rev. Lett.* **5**, 576 (1960).
- ²⁸ Lindenbaum, Love, Niederer, Ozaki, Russel, and Yuan, *Phys. Rev. Lett.* **7**, 352 (1961).
- ²⁹ von Dardel, Dekkers, Mermod, Vivargent, Weber, and Winter, *Phys. Rev. Lett.* **8**, 173 (1962).
- ³⁰ Cook, Keefe, Kerth, Murphy, Wenzel, and Zipf, *Phys. Rev. Lett.* **7**, 182 (1961).
- ³¹ K. Winter, *Intern. Conf. on Theoretical Aspects of Very High-Energy-Phenomena*, CERN, 1961, p. 145.
- ³² V. S. Barashenkov, *Joint Institute for Nuclear Research, Preprint P-187*, 1961; V. G. Grishin, *JETP* **35**, 501 (1958), *Soviet Phys. JETP* **8**, 345 (1959).
- ³³ Bayukov, Birger, Leksin, and Suchkov, *JETP* **43**, 339 (1962), *Soviet Phys. JETP* **16**, 243 (1963).
- ³⁴ Cork, Wenzel, and Causey, *Phys. Rev.* **107**, 859 (1957).
- ³⁵ Cocconi, Diddens, Lillethun, Manning, Taylor, Walker, and Wetherell, *Phys. Rev. Lett.* **7**, 450 (1961).
- ³⁶ Smith, Courant, Fowler, Kraybill, Sandweiss, and Taft, *Proc. of the 1960 Ann. Intern. Conf. of High-Energy Physics at Rochester*, p. 203.
- ³⁷ Preston, Wilson, and Street, *Phys. Rev.* **118**, 579 (1960).
- ³⁸ Do, Kirillova, Markov, Popova, Silin, Tsyganov, Shafronova, Shakhbazyan, and Yuldashev, *JETP* **41**, 1748 (1961), *Soviet Phys. JETP* **14**, 1243 (1962).
- ³⁹ Cvijanovic, Egli, Koch, Nikolic, Schneeberger, Winzeler, Czapek, and Kellner, *Proc. Aix-en-Provence Intern. Conf. on Elementary Particles*, 1961, p. 111.
- ⁴⁰ Dodd, Jobs, Kinsen Tallini, French, Sherman, Skillicorn, Davies, Derrick, and Radojicic, *Proc. Aix-en-Provence Intern. Conf. on Elementary Particles*, 1961, p. 433.
- ⁴¹ Bayukov, Leksin, and Shalamov, *JETP* **41**, 1025 (1961), *Soviet Phys. JETP* **14**, 729 (1962).
- ⁴² Kotenko, Kuznetsov, Merzon, and Sharov, *JETP* **42**, 1158 (1962), *Soviet Phys. JETP* **15**, 300 (1962).
- ⁴³ R. G. Thomas, *Phys. Rev.* **120**, 1015 (1960).
- ⁴⁴ Wang, Wang, Ting, Ivanov, Katyshev, Kladrnitskaya, Kulyukina, Nguyen, Nikitin, Otwinowski, Solov'ev, Sosnowski, and Shafranov, *JETP* **38**, 426 (1960), *Soviet Phys. JETP* **11**, 313 (1960).
- ⁴⁵ Aïnutdinov, Zombkovskii, Nikitin, and Selektor, *JETP* **42**, 1495 (1962), *Soviet Phys. JETP* **15**, 1038 (1962).
- ⁴⁶ Armenteros, Coombes, Cook, Lambertson, and Wenzel, *Phys. Rev.* **119**, 2068 (1960).
- ⁴⁷ Longo, Helland, Hess, Moyer, and Perez-Mendez, *Phys. Rev. Lett.* **3**, 568 (1959).
- ⁴⁸ Vovenko, Golovanov, Galakhov, Lyubimov, Matulenko, Savin, and Smirnov, *Joint Institute for Nuclear Research, Preprint R-805*, 1961.
- ⁴⁹ Kaplon, Klose, Ritson, and Walker, *Phys. Rev.* **91**, 1573 (1953).
- ⁵⁰ K. P. Ryzhkova and L. I. Sarycheva, *JETP* **28**, 618 (1955), *Soviet Phys. JETP* **1**, 572 (1955).
- ⁵¹ Bozoki, Fenyves, Sandor, Balea, Batagui, Friedlander, Betev, Kavlov, and Mitrani, *JETP* **41**, 1043 (1961), *Soviet Phys. JETP* **14**, 743 (1962).
- ⁵² J. Duthie, *Preprint Kioto Conference*, 1961, Part III.
- ⁵³ Duthie, Fisher, Fowler, Kaddoura, Perkins, and Pinkau, *Phil. Mag.* **6**, 89 (1961).
- ⁵⁴ Grigorov, Murzin, and Rapoport, *JETP* **34**, 506 (1958), *Soviet Phys. JETP* **7**, 348 (1958).
- ⁵⁵ G. T. Zatsepin, *JETP* **19**, 1104 (1949).
- ⁵⁶ N. L. Grigorov, *UFN* **58**, 599 (1956).
- ⁵⁷ Grigorov, Shestoperov, Sobinyakov, and Podgurskaya, *JETP* **33**, 1099 (1957), *Soviet Phys. JETP* **6**, 848 (1958).
- ⁵⁸ Dovzhenko, Zatsepin, Murzina, Nikol'skii, and Yakovlev, *Proc. Moscow Cosmic-Ray Conference*, 1959, Vol. II, p. 134.
- ⁵⁹ Duthie, Fowler, Kaddoura, Perkins, and Pinkau, *Nuovo cimento* **24**, 122 (1962).
- ⁶⁰ Fukui, Hasegawa, Matano, Miura, Oda, Ogita, Suga, Tanahashi, and Tanako, *Proc. Moscow Cosmic-Ray Conf.*, 1959, Vol. II, p. 30.
- ⁶¹ Vernov, Khristiansen, Belyaeva, Dmitriev, Kulikov, Negin, Solov'eva, and Khrenov, *Izv. AN SSR, ser. Fiz.* **26**, 651 (1962), *Columbia Tech. Transl.* p. 650.
- ⁶² Grigorov, Guseva, Dobrotin, Kotel'nikov, Murzin, Ryabikov, and Slavatinskiĭ, *Proc. Moscow Cosmic-Ray Conf.*, Vol. I, p. 43.
- ⁶³ N. L. Grigorov and V. Ya. Shestoperov, *JETP* **34**, 1539 (1958), *Soviet Phys. JETP* **7**, 1061 (1958).
- ⁶⁴ Citron, quoted by Cranshaw et al., *Phil. Mag.* **3**, 811 (1958).
- ⁶⁵ F. J. M. Farley and J. R. Storey, *Proc. Phys. Soc.* **B70**, 840 (1957).
- ⁶⁶ Harwell and Culham, cited by Cranshaw et al., *Phil. Mag.* **3**, 811 (1958).

- ⁶⁷G. W. Clark, *Phys. Rev.* **108**, 450 (1957); Clark, Kraushaar, Linsley, Rossi, Scherb, *Nature* **180**, 353 (1957).
- ⁶⁸B. Rossi, *Proc. Moscow Cosmic-Ray Conf.*, 1959, Vol. II, p. 18.
- ⁶⁹Delvaille, Kendziorski, and Greisen, *Proc. Moscow Cosmic-Ray Conf.*, 1959, Vol. II, p. 79.
- ⁷⁰Kulikov, Nesterova, Nikol'skii, Solov'eva, Christiansen, and Chudakov, *Proc. Moscow Cosmic-Ray Conf.*, 1959, Vol. II, p. 85.
- ⁷¹J. Malos, *Proc. Moscow Cosmic-Ray Conf.*, 1959, Vol. II, p. 84.
- ⁷²A. E. Brenner and R. W. Williams, *Phys. Rev.* **106**, 1020 (1957).
- ⁷³Bozoki, Fenyves, and Janossy, *Nuclear Phys.* **24**, 412 (1961).
- ⁷⁴K. I. Alekseeva and N. L. Grigorov, *JETP* **35**, 599 (1958), *Soviet Phys. JETP* **8**, 416 (1959).
- ⁷⁵Babayan, Grigorov, Dubrovin, Mishchenko, Murzin, Sarycheva, Sobinyakov, and Rapoport, *Proc. Moscow Cosmic-Ray Conf.*, 1959, Vol. II, p. 174.
- ⁷⁶Ashmore, Cocconi, Diddens, and Wetherell, *Phys. Rev. Lett.* **5**, 576 (1960).
- ⁷⁷Coor, Hill, Hornyak, Smith, and Snow, *Phys. Rev.* **98**, 1369 (1955); P. H. Barrett, *Phys. Rev.* **114**, 1374 (1959); Arkinson, Hess, Perez-Mendez, and Wallace, *Phys. Rev. Lett.* **2**, 168 (1959).
- ⁷⁸J. Duthie, Ph.D. Thesis, University of Bristol, 1961, quoted by D. H. Perkins, *Proc. of Conf. held at CERN June 5-9, 1961*, p. 99.
- ⁷⁹Bowler, Duthie, Fowler, Kaddoura, and Perkins, *Preprint Kyoto Conference, 1961*, p. 3.
- ⁸⁰Brisbout, Gauld, McCusker, Malos, Nishikawa, Peak, and Van Loow, *Preprint Kyoto Conference, 1961*, p. 3.
- ⁸¹Barkow, Chamony, Haskin, Lohrman, Jain, Teucher, and Schein, *Phys. Rev.* **122**, 617 (1961).
- ⁸²Lohrman, Teucher, and Schein, *Phys. Rev.* **122**, 672 (1961).
- ⁸³Bricman, Csejthey-Barth, Lagnaux, and Sacton, *Nuovo cimento* **20**, 1017 (1961).

Translated by E. Marquit